Direct Electrolytic Preparation of RENi$_{5-x}$Al$_x$ (RE = La, Ce, Pr, and Nd) from Rare-Earth Oxides in Molten CaCl$_2$-NaCl

Qiushi Song[1], Qian Xu[1,], Shuang Li[1], Yang Qi[2], Zhiqiang Ni[1], Kai Yu[1]*

[1] School of Materials Science and Metallurgy, Northeastern University, Shenyang 110819, PR China
[2] College of Science, Northeastern University, Shenyang 110819, PR China
[*]E-mail: qianxu201@mail.neu.edu.cn

RENi$_{5-x}$Al$_x$ compounds (RE = La, Ce, Pr, and Nd) were successfully prepared by electro-deoxidation of a solid mixture of NiO, Al$_2$O$_3$, and commercial rare-earth powders in molten LiCl-KCl eutectic at 650 ℃. The reduction pathway was investigated. The cathodic products were analyzed using X-ray diffraction spectroscopy and scanning electron microscopy. The results showed that RENi$_{5-x}$Al$_x$ ($0 \leq x \leq 0.75$) compounds could be obtained by electro-deoxidation in molten salt. The products consisted of interconnected nodular-shaped particles, and the size increased with the Al content in the compounds. The reduction sequence was determined to be Ni, Al, and rare-earth metals. Al-Ni alloys would be formed instead of RENi$_{5-x}$Al$_x$ when excessive Al$_2$O$_3$ was added into the precursors.

1. INTRODUCTION

Over the last decades, RENi$_5$ (RE donates La, Ce, Pr, Nd, Gd, Mm, etc) intermetallic compounds have been widely investigated as anode materials of Ni-MH batteries for the excellent properties of forming rechargeable metal hydrides, because of attractive hydrogen storage characteristics such as high volumetric storage density, moderate plateau pressures, and easy activation [1-6]. The substitution of Ni by other metals such as Al, Mn, Co, Ti, Cr, Fe, and Cu in RENi$_5$ is usually attempted since it can drastically promote hydrogen storage capacity and thermodynamic properties of the prototype RENi$_5$-hydrogen system [7-11]. At present, RENi$_5$-type compounds are commonly prepared in a complicated method, which involves several steps of melting, alloying, casting, annealing and making into powders [3, 12-14]. Furthermore, high purity metals are usually

used as raw materials. These make the compounds less cost effective and slow in production for extensive application.

Electrolytic reduction of pure or mixed oxide powders in molten salt offers a more economical and easier way to prepare metals and alloys. It has been proved to be a feasible way to produce $RENi_5$. Qiu et al. [15] prepared $TbNi_5$ from Tb_4O_7 and NiO mixed powders in molten $CaCl_2$ at 850 ℃, and also investigated the reduction mechanism. Ji et al. [16] obtained $NdNi_5$ by direct electrochemical reduction of a mixture of Nd_2O_3 and NiO in molten $LiCl$. Zhu et al. [17] achieved electrolytic preparation of $LaNi_5$ hydrogen storage powder and evaluated its hydrogen storage performance. Zhao et al. [18] reported electrochemical preparation of $CeNi_5$, and studied the effect of process parameters, such as sintering temperature, cell voltage, and temperature of the molten salt. Kang et al [19, 20] prepared of $LaNi_5$ and $CeNi_4Cu$ by the substitution of Cu. Moreover, some research groups also obtained Ce, $CeNi_5$, $La_xCe_{1-x}Ni_5$, and Nd-Ni electrochemically in molten salt [21-24].

However, most of the previous studies focused on preparation of the $RENi_5$ compounds involving individual rare earth metal from pure oxides. From the viewpoint of practical applications, the utilization of unrefined rare-earth oxides to prepare $RENi_5$ compounds is desirable, which is more competitive in reducing cost reduction. In particular, the superiority of synthesis of RE-Ni-metal compounds by electrolytic reduction in molten salt is usually neglected, even though it could obtain ternary compounds directly from their mixed oxides.

In this study, a commercial product of rare-earth (including La, Ce, Pr, and Nd) oxide mixture (RE_xO_y) was used as the raw material to prepare $RENi_5$ by electrochemical reduction in molten LiCl-KCl eutectic, and the substitution of Ni by Al was performed by adding Al_2O_3 into the cathodic pellets. Additionally, the reaction mechanism of was also discussed.

2. EXPERIMENTAL

The RE_xO_y powder employed in this work was commercial product from Inner Mongolia Baotou Steel Rare-Earth Hi-Tech Co. Ltd., China. All other chemicals were of analytical grade purchased from Tianjin Kemel Co. Ltd., China. The RE_xO_y and NiO powders (RE : Ni = 1 : 1 in molar ratio) were ball milled at about 400 rpm for 4 h. About 1.0 g of the mixture was weighed and compacted into cylindrical pellets (15 mm in diameter and 1.5 mm in thickness) under 10 MPa, and then sintered at 1150 ℃ in air for 4 h. Similarly, pellets with different content of Al_2O_3 were fabricated.

An alumina crucible (inner height: 10 cm, inner diameter: 9 cm) was filled with approximately 400 g of an anhydrous LiCl and KCl eutectic mixture, and placed at the bottom of a tubular stainless steel reactor. The upper end of the reactor was sealed with a stainless steel plate, and argon gas circulation was provided. The reactor was maintained at about 300 ℃ for at least 24 h to remove the moisture, and then heated to 650 ℃ at a rate of about 100 ℃ per hour.

In electrochemical experiments, high density graphite rods (12 mm in diameter and 70 mm in length) and the sintered pellets were used as anode and cathode, respectively, both of which were contacted to a Ni wire (2 mm in diameter), serving as lead wires. A constant voltage of 3.5 V was

applied between the cathode and anode at 650 ℃. Incompletely and completely reduced specimens were obtained by terminating the electrolysis for various durations. The current was recorded as a function of time. Then, the reactor was cooled down to room temperature. The samples were vigorously rinsed with tap water and dried for examinations.

Phase composition of all the samples was determined through a D/Max-2500PC X-ray diffractometer (XRD) with Cu-Kα radiation (λ =1.5405 $\overset{\circ}{A}$). Morphology of the samples was investigated by means of a SSX-550 scanning electron microscope (SEM) equipped with energy-dispersive X-ray analysis (EDX). Chemical composition of rare earth oxides was analyzed by X-ray flourescence spectrometry (XRF).

3. RESULTS AND DISCUSSION

XRF measurement of the as received RE_xO_y powder was performed, and approximate chemical composition of the powder is presented in Table 1. It can be seen that La_2O_3, CeO_2, Pr_6O_{11}, and Nd_2O_3 are the major components, whose total concentration is up to 96 %. Some other elements, such as Si, Al, Fe, Ca, Mg, S, and F, were also detected.

Table 1. Major elemental concentration of RE_xO_y powder examined by XRF

Composition	Concentration (%)	Composition	Concentration (%)
La_2O_3	26.6702	SiO_2	0.1162
CeO_2	50.8855	MgO	0.0518
Pr_6O_{11}	4.4051	Al_2O_3	0.0686
Nd_2O_3	13.7745	SO_3	0.0686
Fe_2O_3	0.1030	F	3.6284
CaO	0.2283		

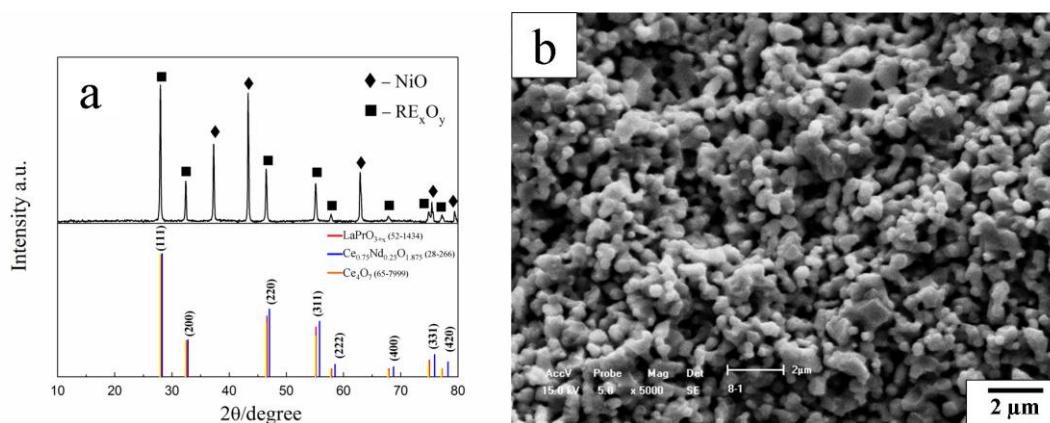**Figure 1.** (a) XRD pattern of RE_xO_y-Ni pellet sintered at 1150 ℃ for 4 h and characteristic peaks of Ce_4O_7, $Ce_{0.25}Nd_{0.75}O_{1.875}$ and $LaPrO_{3+x}$ indexed in JCPDS cards; (b) SEM image of RE_xO_y-Ni sintered pellet at 1150 ℃ for 4 h.

Fig. 1a shows XRD pattern of the RE_xO_y-NiO pellet sintered at 1150 ℃ for 4 h. Several diffraction peaks can be observed besides the peaks of NiO. Ce_4O_7, $Ce_{0.25}Nd_{0.75}O_{1.875}$ and $LaPrO_{3+x}$ with similar crystal structures were indexed in the Joint Committee on Powder Diffraction Standards (JCPDS) cards. Therefore, the undefined peaks should be attributed to coupling effect of the characteristic peaks of these phases. The XRD pattern reveals that new phase has not yielded in the sintering process. Fig. 1b illustrates morphology of the sintered pellet, typically containing particles about 1 μm in diameter. Adequate porosity exists between the particles, which is favorable for the penetration of molten salt in the process of electrochemical reduction.
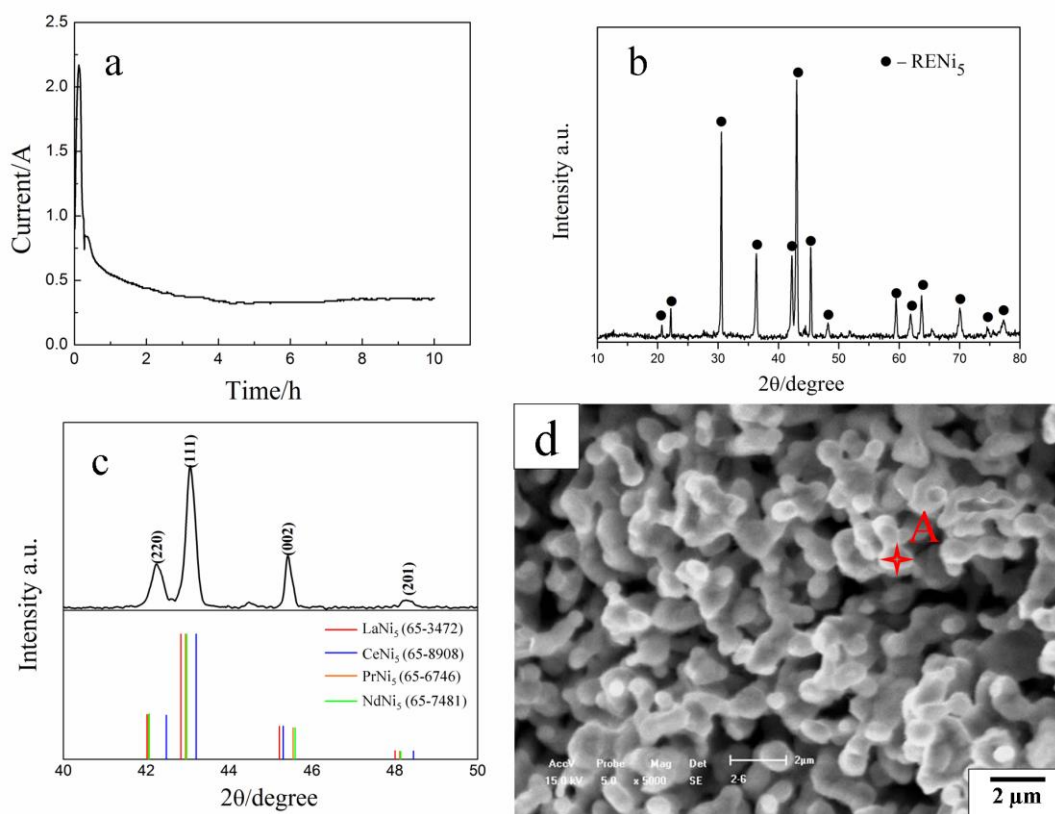

Figure 2. (a) Current vs. time curve recorded during electrochemical reduction of RE_xO_y under 3.5 V for 10 h; (b) XRD; (c) Detailed XRD patterns; (d) SEM image of the sample reduced under 3.5 V for 10 h.

Fig. 2a exhibits a typical current versus time curve recorded during the electro-deoxidation under 3.5 V for 10 h. The plot commences with a current peak of significant magnitude that extends over about 4 h. Thereafter, the current remains relatively small and does not vary markedly as a function of time. Fig. 2b gives XRD pattern of the product after the electro-deoxidation, in combination with the JCPDS reference peaks of $LaNi_5$, $CeNi_5$, $PrNi_5$, and $NdNi_5$. The locations of the characteristic peaks for these compounds are enveloped by the plot examined by XRD, as indicated by the detailed pattern in Fig.2c. It implies that the electrolytic product should be $RENi_5$ compounds, in which the RE is composed of La, Ce, Pr and Nd. Fig.2d denotes SEM image of the reduction product,

which consists of interconnected nodular shape particles with an average size of about 1 μm. EDX analysis of region "A" displayed in Table 2 confirms that La, Ce, Pr, Nd, and Ni are predominant composition in the particles, and the rare-earth metals to Ni ratio is approximately 5.6. From the results put forward above, it could be concluded that $RENi_5$ compounds has been successfully prepared by electro-deoxidation of RE_xO_y. Furthermore, the current efficiency was also considered by calculating the ratio of theoretical quality of the electricity for reduction of cathodic pellet to actual quality of the electricity consumed in electrolytic process. The result is about 9.4 %, which is not a satisfactory value from the perspective of energy consumption.

Table 2. EDX analysis of regions "A" in Fig. 2d and "B", "C", "D" in Fig. 5a-c

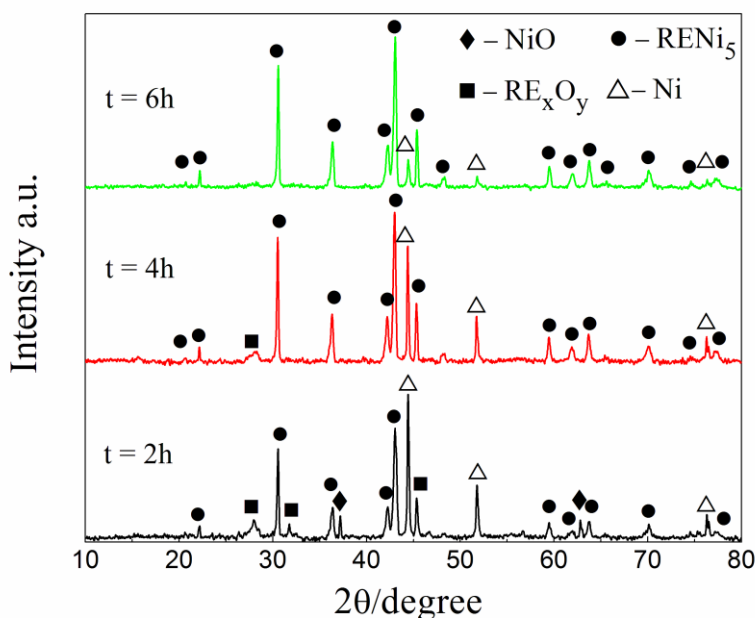| Region	La (at %)	Ce (at %)	Pr (at %)	Nd (at %)	Ni (at %)	Al (at %)
A	3.8	8.8	0.5	1.5	85.4	
B	4.8	9.7	1.8	2.9	77.2	3.6
C	3.2	8.9	0.6	2.4	78.1	6.8
D	3.3	8.9	0.9	2.3	64.8	19.8

Figure 3. XRD patterns of the samples obtained for 2, 4, and 6 h under 3.5 V.

In order to investigate reaction pathway of the reduction, electrochemical experiments were carried out with various durations ranging from 2 to 6 h. Fig. 3 gives XRD patterns of samples obtained for different durations. The sample recovered after 2 h of reduction was found to consist of $RENi_5$, Ni, RE_xO_y, and NiO. When the reduction time was prolonged to 4 h, Ni and $RENi_5$ were the primary phases, and a small quantity of RE_xO_y was also detected. In addition, NiO can be hardly observed. After 6 h of electrolysis, $RENi_5$ became the overwhelming phase besides a small amount of

Ni. The results confirm that the reduction of NiO to Ni is more favorable than that of RE_xO_y, as discussed in the literature [15, 18, 19]. Subsequently, $RENi_5$ would be formed once the recovery of rare earth metals occurred. Therefore, the evolution of current in Fig. 2a could be explained. Electrolytic reduction of nickel and rare earth oxides took place prevailingly in the period of 0 - 4 h, corresponding to the current peak in the current versus time plot, Then electrochemical removal of oxygen from the cathode became a less dominant process. Meanwhile, the background current contributed significantly to the recorded current, which may lead relatively low overall current efficiency of less than 10 percent. Another issue with respect to the unsatisfactory current efficiency is that carbon powder stripped from graphite anode was found to float in the molten salt at the late period of experiment, which may cause short circuit of the electrolytic cell. It should be mentioned that rare-earth oxychlorides such as LiOCl and CeOCl did not appear during the electrolysis, which are common intermediates during electrolytic reduction of rare-earth oxides in molten salt [15, 18, 19]. This is probably due to relatively low working temperature of the electro-deoxidation, which is inadequate for the diffusion of chloride ions into RE_xO_y to form REOCl [20].
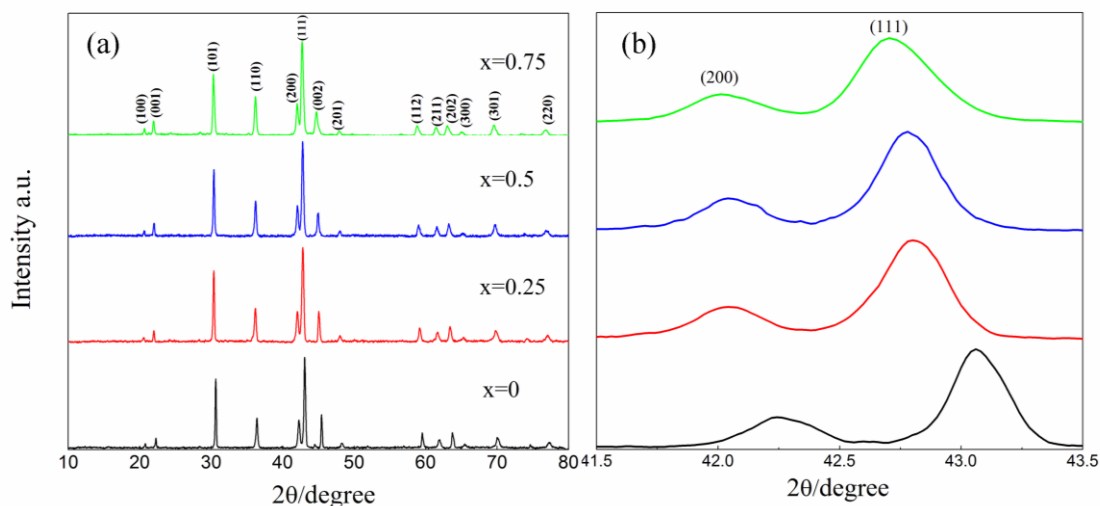

Figure 4. (a) XRD; (b) Detailed XRD patterns of $RENi_{5-x}Al_x$ (x= 0, 0.25, 0.5, 0.75) prepared by electro-deoxidation under 3.5 V for 12 h.

A set of experiments were carried out to investigate the feasibility of preparation of $RENi_{5-x}Al_x$ in the electrochemical method by mixing Al_2O_3 powder into the sintered pellets. Fig. 4a shows XRD patterns of the samples produced electrochemically from the sintered precursors with the Al to Ni molar ratio varying from 0 : 5 to 0.75 : 4.25, showing partial substitution of Ni by Al in the $RENi_5$ structure. Fig. 4b illustrates the detailed patterns of (200) and (111) peaks. The peaks shift to low angle positions with increasing of Al content, which provides evidence for the enhancement of both the cell parameters (a, c) and cell volume (V), as exhibited in Table. 3. These results are ascribed to the relatively larger radius of Al atom (1.43 Å) than that of Ni atom (1.23 Å) [25].

Table 3. Lattice parameters and cell volume of $RENi_{5-x}Al_x$ ($x = 0 - 0.75$)

Samples	a (Å)	c (Å)	V (Å^3)
$RENi_5$	4.938	3.990	84.24
$RENi_{4.75}Al_{0.25}$	4.962	4.025	85.80
$RENi_{4.5}Al_{0.5}$	4.961	4.036	86.02
$RENi_{4.25}Al_{0.75}$	4.966	4.054	86.59

Figs. 5(a)-(c) are SEM images of $RENi_{4.25}Al_{0.75}$ $RENi_{4.5}Al_{0.5}$ and $RENi_{4.25}Al_{0.75}$, respectively. The products are composed of interconnected nodular-shaped particles, whose morphologies present little difference from that of the particles without the participation of Al. But the particle size increases with the amount of Al doped into $RENi_{5-x}Al_x$. EDX analysis was performed for different regions, as displayed in Table 2. It verifies that the trend of sizes variation is in agreement with the Al content in the particles.
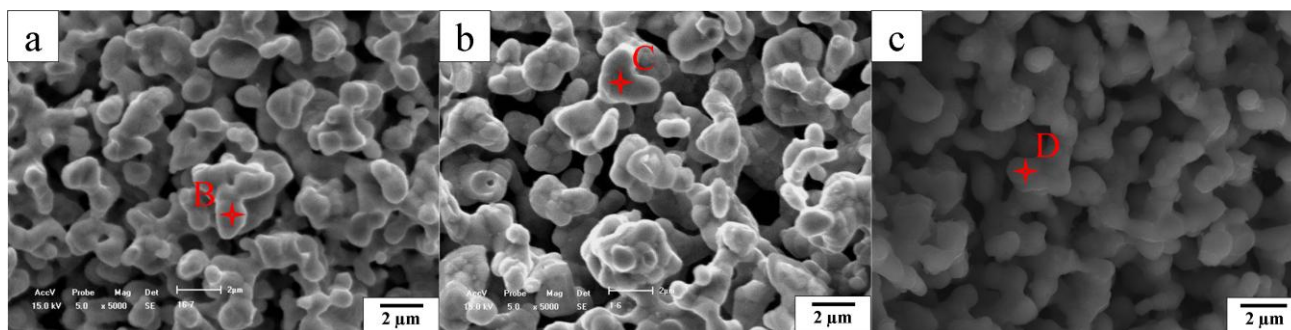
Figure 5. SEM images of $RENi_{5-x}Al_x$ (a) x=0.25; (b) x=0.5; (c) x=0.75 prepared by electro-deoxidation under 3.5 V for 12 h.

However, a single phase of $RENi_{5-x}Al_x$ product could not be obtained once the molar ratio of Ni to Al was higher than 0.75 : 4.25. Then, Al-Ni alloys and rare-earth oxides were gradually observed in the samples, as can be seen in Fig. 6. When initial molar ratio of Al to Ni in sintered precursor was 1 : 4, Al-Ni alloys including AlNi and $AlNi_3$ appeared besides $RENi_{5-x}Al_x$, and the unreduced rare earth oxide of Pr_2O_3 also existed in the product. AlNi became dominant component of the product once more Al was added into the cathodic pellets. Moreover, other rare-earth oxides such as Ce_4O_7 and Ce_2O_3 were visible. This phenomenon is probably related to the priority of the reactions occurred during the electrolytic reduction process.
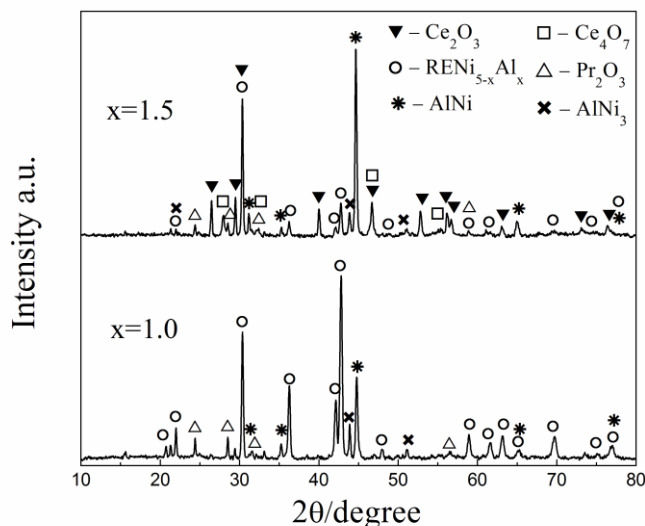
Figure 6. XRD patterns of the samples prepared by electro-deoxidation with the Al to Ni ratio of 1:4 and 1.5 : 3.5 in sintered pellets.

Table 4. Thermodynamic calculations of the reactions during electrochemical reduction at 650 ℃

Reaction	ΔG^o (KJ · mol^{-1})	ΔE^o (V)
$NiO = Ni + 0.5O_2(g)$	154.4	0.80
$Al_2O_3 = 2La + 1.5O_2(g)$	1383.6	2.39
$La_2O_3 = 2La + 1.5O_2(g)$	1528.4	2.64
$CeO_2 = Ce + O_2(g)$	895.4	2.32
$Pr_6O_{11} = 6Pr + 5.5O_2(g)$	4648.7	2.19
$Nd_2O_3 = 2Nd + 1.5O_2(g)$	1545.7	2.67
$C + O_2(g) = CO_2(g)$	-395.7	
$Al + Ni = AlNi$	-111.3	
$Al + 3Ni = AlNi_3$	-144.2	
$La + 5Ni = LaNi_5$	-23.2	

Table 4 demonstrates thermodynamic calculations of the possible reactions during the electro-deoxidation at 650 ℃. The theoretical decomposition voltage of NiO is 0.80 V, so it would be electro-deoxidized preferentially when a voltage of 3.5 V was applied. Although the decomposition voltage of Al₂O₃ does not clarify obvious superiority in comparison with rare earth oxides from thermodynamic considerations, it can be predicted that the reduction of Al is more favorable than that of rare-earth metals, as described in the literature [15, 19]. Additionlly, Ni would react with Al spontaneously to form the Al-Ni alloys of AlNi and Al₃Ni. Therefore, the reduction of rare earth oxides is a relatively tougher process with the absence of Ni, which could promote the recovery of rare-earth metals by forming RENi₅ compounds. And the existence of rare-earth oxides in the products can be explained.

The limitation of Al substitution was also considered from the viewpoint of structure. Fig. 7 shows the crystal structure schematics of $RENi_{5-x}Al_x$ (RE = La, Ce, Pr, and Nd). All the ternary compounds crystallize in $CaCu_5$ type hexagonal structure (space group, *P6/mmm*). The structure of $RENi_5$ consists of two distinct layers of atoms. The basal layer contains relatively larger atoms of RE at 1a (0, 0, 0) sites, and smaller atoms of Ni at 2g (1/3, 2/3, 0) sites. The middle layer only contains Ni atoms at (1/2, 0, 1/2) sites. The replacement of Ni atoms by Al occurred in the middle layer (3g sites) preferentially instead of Ni atoms in the basal layer, when the amount of Al was inadequate (x ≤ 0.25) during the preparation of the ternary compounds. Then 3c sites were available once the amount of Al was large enough (x ≥ 0.5) for the substitution. However, $RENi_{4.25}Al_{0.75}$ seems to be the terminal product of the $RENi_{5-x}Al_x$ species produced by electro-deoxidization in molten salt even if excess Al was mixed into the cathodic pellets. This is probably because of excessive crystal stress in the structure, which is inevitably generated owing to diverse radii of Ni and Al atoms. Nevertheless, the activation energy provided by the environment in molten salt may restrict further combination of $RENi_{5-x}Al_x$ once the molar ratio of Al to Ni exceeded 0.75 : 4.25.
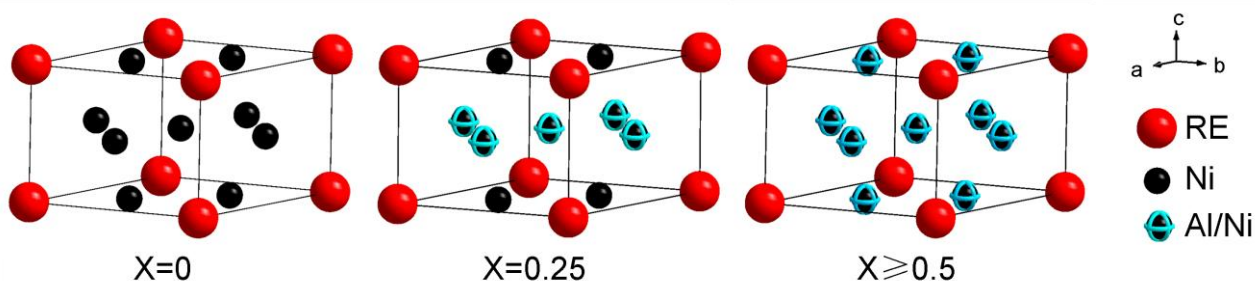

Figure 7. Schematic illustration of the crystal structures of $RENi_{5-x}Al_x$ (RE = La, Ce, Pr and Nd) with various molar ratio of Al to Ni.

4. CONCLUSIONS

$RENi_5$ (RE = La, Ce, Pr, and Nd) compounds were electrochemically prepared from commercial rare-earth oxides and analytical grade NiO under 3.5 V in molten LiCl-KCl at 650 ℃. The product was composed of interconnected nodular-shaped particles with an average size of about 1 μm. During the elecro-deoxidation, Ni was preferentially reduced compared with rare-earth metals. Rare earth oxychlorides did not appear in this process. The feasibility to synthesize partially replaced compounds of $RENi_{5-x}Al_x$ was attempted. The morphology of the products changed little in comparison with that without substitution, but the particles size increased with the amount of Al substitution. The reduction of Al occurred prior to that of rare-earth metals. The present experimental conditions restricted molar ratio of Al content in $RENi_{5-x}Al_x$ less than 0.75. Al-Ni alloys of AlNi and $AlNi_3$ would emerge in the product once excess Al was added into the precursor, and the formation of $RENi_{5-x}Al_x$ was restrained.

References

1. M.H. Mendelsohn, D.M. Gruen and A.E. Dwight, *J. Less-Common Met.*, 63 (1979) 193.
2. K. Yamaguchi, D.Y. Kim, M. Ohtsuka and K. Itagaki, *J. Alloys Compd.*, 221 (1995) 161.
3. M. Tliha, H. Mathlouthi, J. Lamloumi and A. Percheron-Guegan, *J. Alloys Compd.*, 436 (2007) 221.
4. M.S. Balogun, Z.M. Wang, H.X. Chen, J.Q. Deng, Q.R. Yao and H.Y. Zhou, *Int. J. Hydrogen Energy*, 38 (2013) 10926.
5. S.Q. Yang, S.M. Han, Y. Li and J.J. Liu, *Mater. Sci. Eng. B*, 178 (2013) 39.
6. L. Shcherbakova, M. Spodaryk and Y. Solonin, *Int. J. Hydrogen Energy*, 38 (2013) 12133.
7. G.I. Miletic and Z. Blazina, *J. Alloys Compd.*, 335 (2002) 81.
8. J. Liu, Y.F. Yang and H.X. Shao, *J. Alloys Compd.*, 429 (2007) 285.
9. J. Liu, Y.F. Yang, Y. Li, P. Yu, Y.H. He and H.X. Shao, *Int. J. Hydrogen Energy*, 32 (2007) 1905.
10. Y. Q. Lei, J.J. Jiang, D.L. Sun, J. Wu and Q.D. Wang, *J. Alloys Compd.*, 231 (1995) 553.
11. S.L. Li, P. Wang, W. Chen, G. Luo, D.M. Chen and K. Yang, *J. Alloys Compd.*, 485 (2009) 867.
12. J. Matsuda, Y. Nakamura and E. Akiba, *J. Alloys Compd.*, 509 (2011) 7498.
13. H.H. Cheng, H.G. Yang, S.L. Li, X.X. Deng, D.M. Chen and K. Yang, *J. Alloys Compd.*, 458 (2008) 330.
14. H. Senoh, N. Takeichi, H.T. Takeshita, H. Tanaka, T. Kiyobayashi and N. Kuriyama, *Mater. Sci. Eng. B*, 108 (2004) 96.
15. G.H. Qiu, D.H. Wang, X.B Jin and G.Z. Chen, *Electrochim. Acta*, 51 (2006) 5785.
16. H.S. Ji, H.Y. Ryu, S.M. Jeong and S.W. Cho, *Chem. Lett.*, 42 (2010) 1182.
17. Y. Zhu, D.H. Wang, M. Ma, X.H. Hu, X.B. Jin and G.Z. Chen, *Chem. Commun.*, (2007) 2515.
18. B.J Zhao, L. Wang, L. Dai, G.H. Cui, H.Z. Zhou and R.V. Kumar, *J. Alloys Compd.*, 468 (2009) 379-385.
19. X. Kang, Q. Xu, S.J. Ma, L.N. Zhao and Q.S. Song, *Electrochemistry*, 77 (2009), 1.
20. X. Kang, Q. Xu, X.M. Yang and Q.S. Song, *Mater. Lett.*, 64 (2010) 2258.
21. B. Claux, J. Serp and J. Fouletier, *Electrochim. Acta*, 55 (2011) 2771.
22. K. Yasuda, S. Kobayashi, T. Nohira and R. Hagiwara, *Electrochim. Acta*, 92 (2013) 349.
23. B.J. Zhao, X.G. Lu, Q.D. Zhong, C.H. Li and S.L. Chen, *Electrochim. Acta*, 55 (2010) 2996.
24. B.J. Zhao, X.G. Lu, C.H. Li and Q.D. Zhong, *Acta Metall. Sin.*, 45 (2009) 1255.
25. J. Liu, Y.F. Yang, P. Yu, Y. Li and H.X. Shao, *J. Power Sources*, 161 (2006) 1435.